

# Overexpression of Diacylglycerol Kinase $\eta$ Enhances $G\alpha_q$ -Coupled G Protein–Coupled Receptor Signaling<sup>§</sup>

Joseph E. Rittiner, Victoria E. Brings, and Mark J. Zylka

Department of Cell Biology and Physiology, University of North Carolina Neuroscience Center, University of North Carolina, Chapel Hill, North Carolina

Received December 11, 2013; accepted March 7, 2014

## ABSTRACT

Multiple genome-wide association studies have linked diacylglycerol kinase  $\eta$  (DGK $\eta$ ) to bipolar disorder (BPD). Moreover, DGK $\eta$  expression is increased in tissue from patients with BPD. How increased levels of this lipid kinase might affect cellular functions is currently unclear. Here, we overexpressed mouse DGK $\eta$  in human embryonic kidney 293 cells to examine substrate specificity and signaling downstream of endogenous G protein–coupled receptors (GPCRs). We found that DGK $\eta$  can phosphorylate diacylglycerol (DAG) with different acyl side chains (8:0, 12:0, 18:1). In addition, overexpression of DGK $\eta$  enhanced calcium mobilization after stimulating muscarinic receptors with carbachol and after stimulating purinergic receptors with ATP. This effect required DGK $\eta$  catalytic activity, as assessed using a kinase-dead (G389D) mutant and multiple truncation constructs. DGK $\eta$

was localized throughout the cytosol and did not translocate to the plasma membrane after stimulation with carbachol. Since protein kinase C (PKC) can be activated by DAG and promotes receptor desensitization, we also examined functional interactions between PKC and DGK $\eta$ . We found that acute activation of PKC with phorbol 12-myristate 13-acetate shortened carbachol-evoked calcium responses and occluded the effect of overexpressed DGK $\eta$ . Moreover, inhibition of PKC activity with bisindolylmaleimide I (BIM I) produced the same enhancing effect on carbachol-evoked calcium mobilization as overexpressed DGK $\eta$ , and overexpression of DGK $\eta$  produced no additional effect on calcium mobilization in the presence of BIM I. Taken together, our data suggest that DGK $\eta$  enhances GPCR signaling by reducing PKC activation.

## Introduction

Diacylglycerol kinases (DGKs) are a large family of enzymes that catalyze the phosphorylation of the membrane lipid diacylglycerol (DAG) to phosphatidic acid (van Blitterswijk and Houssa, 2000; Sakane et al., 2007). DAG and phosphatidic acid are important second messengers and regulate diverse proteins and pathways, including protein kinase C (PKC) (Mellor and Parker, 1998), ion channels (Lucas et al., 2003), endocannabinoid production (Gregg et al., 2012), and phosphoinositide synthesis (Jenkins et al., 1994). DGKs are thus well positioned to regulate diverse intracellular signaling pathways (Merida et al., 2008).

In recent years, several studies have identified genetic associations between *DGKH* and bipolar disorder (BPD) (Baum et al., 2008; Squassina et al., 2009; Takata et al., 2011; Weber et al., 2011; Yosifova et al., 2011; Zeng et al., 2011). *DGKH* is

the gene that encodes diacylglycerol kinase  $\eta$  (DGK $\eta$ ). In addition, Moya and colleagues found that DGK $\eta$  mRNA was expressed at higher levels in postmortem tissue samples from patients with BPD than unaffected controls (Moya et al., 2010). DGK $\eta$  is a type 2 DGK with two known splice variants (Klauck et al., 1996; Murakami et al., 2003) and was recently implicated in lung cancer (Nakano et al., 2014). However, how alterations in DGK $\eta$  levels might affect cellular functions or contribute to BPD pathogenesis is currently unknown.

Dysregulation of G protein–coupled receptor (GPCR) activity is involved in the pathology of many psychiatric disorders, including BPD (Catapano and Manji, 2007). Indeed, tissues from BPD patients exhibit changes in GPCR (Pantazopoulos et al., 2004) and G protein subunit expression (Young et al., 1993; Rao et al., 2009), enhanced receptor–G protein coupling (Friedman and Wang, 1996), and decreased expression of GPCR kinase 3 (GRK3) (Rao et al., 2009). Furthermore, therapeutic concentrations of lithium and valproate, common treatments of BPD, inhibit G protein activation after GPCR stimulation in cell membranes (Avissar et al., 1988) and platelets from bipolar patients (Hahn et al., 2005).

Given that DGK $\eta$  is expressed at higher levels in BPD patients and has the potential to affect GPCR signaling, we

This work was supported by the National Institutes of Health National Institute of Neurological Disorders and Stroke [Grants R01-NS081127 and R01-NS067688].

dx.doi.org/10.1124/mol.113.091280.

§ This article has supplemental material available at molpharm.aspetjournals.org.

**ABBREVIATIONS:** AUC, area under the curve; BIM I, bisindolylmaleimide I; BPD, bipolar disorder; BSA, bovine serum albumin; Co-IP, coimmunoprecipitation; DAG, diacylglycerol; DGK, diacylglycerol kinase; DTT, DL-dithiothreitol; EGFR, epidermal growth factor receptor; GFP, green fluorescent protein; G $\delta$ 6976, 5,6,7,13-tetrahydro-13-methyl-5-oxo-12H-indolo[2,3-a]pyrrolo[3,4-c]carbazole-12-propanenitrile; GPCR, G protein–coupled receptor; GRK, G protein–coupled receptor kinase; HEK, human embryonic kidney; PA, phosphatidic acid; PBS, phosphate-buffered saline; PCR, polymerase chain reaction; PKC, protein kinase C; PMA, phorbol-12-myristate-13-acetate; RFP, red fluorescent protein; TBST, Tris-buffered saline/Tween 20; WT, wild-type.

sought to determine if overexpression of DGK $\eta$  affected GPCR signaling in human embryonic kidney (HEK) 293 cells, a model cell line with well characterized GPCR signaling cascades (Luo et al., 2008). Here, we found that overexpression of DGK $\eta$  dramatically increased the duration of calcium responses after stimulating endogenous G $\alpha_q$ -coupled GPCRs. The effect of DGK $\eta$  overexpression was dependent on DGK $\eta$  catalytic activity and was blocked by inhibition of PKC. Taken together, our data suggest that DGK $\eta$  enhances GPCR signaling by attenuating PKC activity, possibly by attenuating PKC-dependent receptor desensitization.

## Materials and Methods

Carbamoylcholine chloride (carbachol), D-sorbitol, *n*-butanol, EDTA, phenylmethanesulfonyl fluoride, sodium fluoride, DL-dithiothreitol (DTT), sodium deoxycholate, ATP, HEPES sodium salt, glycerol, sodium pyrophosphate, Dulbecco's phosphate-buffered saline (PBS), fatty acid-free bovine serum albumin (BSA), poly-D-lysine, bromophenol blue, and phorbol 12-myristate 13-acetate (PMA) were purchased from Sigma-Aldrich (St. Louis, MO). Concentrated hydrochloric acid, Tris hydrochloride (Tris-HCl), sodium chloride (NaCl), magnesium chloride hexahydrate (MgCl<sub>2</sub>), SDS, Triton X-100, Tween 20, and D-glucose were purchased from Fisher Scientific (Waltham, MA). Bisindolylmaleimide I (BIM I) was purchased from Cayman Chemical (Ann Arbor, MI). G66976 (5,6,7,13-tetrahydro-13-methyl-5-oxo-12*H*-indolo[2,3-*a*]pyrrolo[3,4-*c*]carbazole-12-propanenitrile) was purchased from Tocris Bioscience (Bristol, UK). BisNonidet P40 substitute (NP40) was purchased from USB Corporation (Cleveland, OH).  $\gamma$ -<sup>32</sup>P-labeled ATP (6000 Ci/mmol, 150 mCi/ml) was purchased from PerkinElmer (Waltham, MA).

**Molecular Biology.** A full-length clone of mouse DGK $\eta$  isoform 1 was generated by polymerase chain reaction (PCR) amplification using cDNA from C57BL/6 mouse neurons as a template (bases 1–3471 from GenBank accession #NM\_001081336.1) (Murakami et al., 2003). The initial clone was found to be unstable due to high GC content at the 5' end of the DGK $\eta$  coding sequence. To remedy this problem, the first 69 bases of the DGK $\eta$  coding sequence were modified to decrease GC content while preserving the wild-type (WT) DGK $\eta$  amino acid sequence (native sequence: ATG GCC GGG GCC GGC AGC CAG CAC CAC CCT CAG GGC GTC GCG GGA GGA GCG GTC GCT GGG GCC AGC GCG; modified sequence: ATG GCA GGA GCA GGA AGT CAG CAT CAT CCT CAG GGA GTT GCA GGA GGA GCA GTT GCA GGA GCA ACT GCA). The resulting construct was stable and was used to generate all subsequent constructs. DGK $\eta$  truncation constructs were generated by PCR amplification. The G389D point mutant was generated by traditional PCR-based mutagenesis. Full-length DGK $\eta$  and all DGK $\eta$  constructs were inserted into the multiple cloning site of pcDNA 3.1(+)-downstream of monomeric red fluorescent protein (RFP) lacking a stop codon to create fusion constructs with N-terminal RFP tags. A DGK $\eta$ -646 $\Delta$  fusion construct with an N-terminal Venus tag was generated in the same fashion. All constructs contained a Kozak consensus sequence and were sequence verified.

**Cell Culture.** HEK293 cells were grown in Dulbecco's modified Eagle's medium (Gibco, Grand Island, NY) containing 10% fetal bovine serum, 100 U/ml penicillin, and 100  $\mu$ g/ml streptomycin at 37°C and 5% CO<sub>2</sub>. Cells were plated on polylysine-coated glass-bottom dishes (MatTek, Ashland, MA) for calcium imaging, polylysine-coated glass coverslips (Brain Research Laboratories, Waban, MA) for immunostaining, and polylysine-coated six-well plates (Corning, Corning, NY) for all other experiments. Twenty-four hours after plating, cells were transfected with Lipofectamine/Plus (Invitrogen, Carlsbad, CA) in serum-free Dulbecco's modified Eagle's medium according to the manufacturer's instructions. Each plate/well was transfected with 500 ng of each DNA construct, and the total amount

of DNA per transfection was normalized to 1  $\mu$ g with empty vector. After 4 hours, the transfection medium was replaced with fresh growth medium. All experiments were performed 24 hours after transfection.

**Calcium Imaging.** Calcium imaging was performed as described previously (Rittiner et al., 2012). Briefly, HEK293 cells expressing various DGK $\eta$  constructs and controls were washed twice in Hanks' balanced salt solution assay buffer (Invitrogen; 140 mg/l CaCl<sub>2</sub>, 100 mg/l MgCl<sub>2</sub>-6H<sub>2</sub>O, 100 mg/l MgSO<sub>4</sub>-7H<sub>2</sub>O, 400 mg/l KCl, 60 mg/l KH<sub>2</sub>PO<sub>4</sub>, 350 mg/l NaHCO<sub>3</sub>, 8 g/l NaCl, 48 mg/l Na<sub>2</sub>HPO<sub>4</sub>, 1 g/l D-glucose, supplemented with 2.4 g/l HEPES, 2 g/l D-glucose, and 0.1% fatty acid-free BSA, pH 7.3) and loaded with 2  $\mu$ M Fura-2 AM (Invitrogen) in 0.02% Pluronic F-127 (Invitrogen) in assay buffer for 1 hour at room temperature. For experiments lacking extracellular calcium, identical assay buffer lacking CaCl<sub>2</sub> was used throughout the procedure. Cells were then washed three times in assay buffer, incubated at room temperature for 30 minutes, and imaged on an Eclipse Ti microscope (Nikon, Tokyo, Japan) at room temperature. A DG-4 light source (Sutter, Novato, CA), CFI Plan Fluor 20 $\times$  objective (Nikon), Clara DR-328G-C01-SIL CCD camera (Andor, Belfast, UK) and NIS Elements imaging software (Nikon) were used to image calcium responses. All experiments used 500-millisecond excitation at 340 nm and 250-millisecond excitation at 380 nm. Fura-2 emission was measured at 510 nm.

Fresh assay buffer was added prior to each experiment. After 40 seconds of baseline imaging, the assay buffer was aspirated and agonist solution was added. All solutions were aspirated and pipetted manually. Aspiration or addition of buffer alone did not cause calcium responses (data not shown, see Fig. 6B, PMA-only trace for equivalent experiment). For PKC inhibition experiments, inhibitor was added in assay buffer 30 minutes prior to imaging and was present in all wash and agonist solutions. Only cells that expressed visible RFP fluorescence, had low baseline Fura-2 ratios (<0.6), and responded to agonist stimulation (Fura-2 ratio > 0.8 at any time after agonist addition) were analyzed. For experiments using cells transfected with RFP-DGK $\eta$ - $\Delta$ 645 and Venus-DGK $\eta$ -646 $\Delta$ , only cells expressing both visible RFP fluorescence and visible Venus fluorescence were analyzed. Real-time response profiles were generated as described previously (Rittiner et al., 2012). Area under curve (AUC) and peak response values were calculated relative to baseline Fura-2 ratios on a cell-by-cell basis and averaged over all cells in each condition. To control for day-to-day variation in calcium responses, control cells expressing RFP alone were tested as part of each experiment. AUC and peak response values were then normalized such that RFP alone was set at a value of 1. To create scatter plots comparing expression and AUC values, RFP-DGK $\eta$  expression levels were calculated for each cell by quantifying RFP fluorescence.

**Confocal Microscopy.** HEK293 cells expressing RFP-DGK $\eta$  were washed twice in Hanks' balanced salt solution assay buffer and imaged using a CSU-10 spinning disc confocal scanner (Yokogawa, Tokyo, Japan) mounted on a TE2000 microscope (Nikon). An Argon/Krypton laser light source, Orca-ER camera (Hamamatsu Photonics, Hamamatsu, Japan), and SimplePCI imaging software (Hamamatsu) were used to image RFP-tagged DGK $\eta$ . After approximately 1 minute of baseline imaging, assay buffer was replaced with buffer containing 10  $\mu$ M carbachol or 500 mM sorbitol, and imaging continued for an additional 15 minutes. Solutions were removed and added by manual pipetting.

**Immunostaining.** HEK293 cells expressing RFP were incubated in PBS alone or 300 nM PMA in PBS for 10 minutes at 37°C, then fixed in ice-cold 4% paraformaldehyde (Fisher Scientific) for 15 minutes. After incubating in 0.5% Triton X-100 in PBS for 15 minutes, coverslips were blocked for 30 minutes in blocking solution—0.1% Triton X-100 and 5% normal goat serum (Invitrogen) in PBS—then incubated with rabbit anti-PKC $\delta$  primary antibody (Santa Cruz Biotechnology, Santa Cruz, CA) in blocking solution overnight at 4°C. Cells were then washed with 10% goat serum in PBS for 30 minutes and incubated in Alexa Fluor 488-conjugated goat anti-rabbit

secondary antibody (Invitrogen) and DRAQ5 nuclear dye (Cell Signaling Technology, Beverly, MA) in blocking solution for 1 hour at room temperature. Cells were washed three times (5 minutes/wash) with PBS between each step. Coverslips were mounted onto microscope slides (Fisher Scientific) with Fluoro-Gel (Electron Microscopy Sciences, Hatfield, PA) and stored at 4°C. Slides were imaged at room temperature the following day on an LSM 510 microscope (Zeiss, Oberkochen, Germany), using multiline Argon and Helium-Neon laser light sources, a 63× objective, and ZEN imaging software (Zeiss).

**In Vitro Kinase Assay.** The DGK in vitro kinase assay was adapted from previous studies (Kanoh et al., 1992; Ohanian and Heagerty, 1994). HEK293 cells expressing RFP-tagged DGK $\eta$  (WT or truncation constructs) or RFP alone were washed twice with ice-cold PBS and scraped into ice-cold lysis buffer—50 mM Tris-HCl pH 7.5, 150 mM NaCl, 1 mM EDTA, 1 mM phenylmethanesulfonyl fluoride, 1× Complete Mini protease inhibitor cocktail (Roche, Basel, Switzerland), 1× Phosphatase Inhibitor Cocktail 2 (Sigma-Aldrich)—to preserve any potential phosphorylation events on protein. Cells were disrupted by brief sonication on ice, and debris was collected by centrifugation at 10,000g for 10 minutes at 4°C. Clarified lysates were kept on ice.

The final reaction mixture contained 50 mM Tris-HCl pH 7.4, 100 mM NaCl, 20 mM NaF, 10 mM MgCl<sub>2</sub>, 1 mM DTT, 1 mM EDTA, 1 mM sodium deoxycholate, 0.5 mM DAG (8:0, 12:0, or 18:1), 1 mM [ $\gamma$ -<sup>32</sup>P]ATP (50  $\mu$ Ci/rxn), and lysate; reaction volume was 50  $\mu$ l. A calculated amount of 1,2-dioctanoyl-glycerol (8:0 DAG), 1,2-dilauroyl-glycerol (12:0 DAG), or 1,2-dioleoyl-glycerol (18:1 DAG) in chloroform (Avanti Polar Lipids, Alabaster, AL) was deposited in a glass tube under a stream of dry nitrogen gas. The DAG was then resuspended in an appropriate amount of 5× kinase buffer (250 mM Tris-HCl pH 7.4, 500 mM NaCl, 100 mM NaF, 50 mM MgCl<sub>2</sub>, 5 mM DTT, 5 mM EDTA) and 10 mM sodium deoxycholate by brief bath sonication. 15  $\mu$ l of the DAG suspension was added to a tube containing 20  $\mu$ l of water, followed by 5  $\mu$ l of 10 mM [ $\gamma$ -<sup>32</sup>P]ATP. The reaction was initiated by adding 10  $\mu$ l of lysate, incubated for 3 minutes at 30°C, and then stopped by adding 25  $\mu$ l of 12 N HCl followed by 750  $\mu$ l of water saturated with *n*-butanol. Lipids were extracted from the reaction mixture by adding 500  $\mu$ l of *n*-butanol, mixing thoroughly, and separating by centrifugation at 1000g for 5 minutes. The organic phase (450  $\mu$ l) was washed with 500  $\mu$ l of *n*-butanol-saturated water and separated by centrifugation, with care taken not to disturb the aqueous phase. Next, 350  $\mu$ l of this organic phase was washed again in the same fashion. Finally, 250  $\mu$ l of the washed organic phase was transferred to a scintillation vial containing 2 ml of ScintiSafe Econo 2 scintillation fluid (Fisher Scientific), mixed gently, and counted on a Wallac Rackbeta 1209 liquid scintillation counter (LKB Instruments, Mount Waverley, VIC, Australia).

For experiments comparing different DGK $\eta$  truncation constructs, each lysate sample was analyzed by anti-RFP western blotting as described below, and the band intensity was quantified using ImageJ image analysis software (NIH, Bethesda, MD). The DGK $\eta$  activity data were corrected for differences in expression, and normalized such that RFP alone was set at a value of 0, and wild-type DGK $\eta$  was set at a value of 1.

**Western Blotting.** A 15- $\mu$ l portion of each lysate used in the in vitro kinase assay was mixed with an appropriate amount of 4× Laemmli sample buffer—125 mM Tris-HCl, 40% (v/v) glycerol, 2% (v/v) SDS, 10% (v/v)  $\beta$ -mercaptoethanol (Bio-Rad, Hercules, CA), 0.02% (w/v) bromophenol blue—and separated by SDS-PAGE on a 4% to 15% gradient gel (Bio-Rad) at 100 V for 1 hour. Proteins were transferred to a polyvinylidene fluoride membrane (Bio-Rad) at 100 V for 70 minutes on ice and blocked with 5% nonfat milk (Bio-Rad) in Tris-buffered saline/Tween 20 (TBST; 100 mM Tris-HCl pH 7.5, 165 mM NaCl, 0.1% Tween 20) for 1 hour at room temperature. Blots were then incubated with rabbit anti-RFP primary antibody (Invitrogen) in 5% BSA (Sigma-Aldrich) in TBST overnight at 4°C. The following day, blots were washed three times (5 minutes/wash) with TBST and incubated with IRDye800-conjugated donkey anti-rabbit secondary antibody (LI-COR, Lincoln, NE) in 5% nonfat milk/TBST for 1.5 hours at room temperature. Blots were then

washed three times (5 minutes/wash) with TBST and imaged on an Odyssey CLx infrared imaging system (LI-COR).

**Coimmunoprecipitation.** HEK293 cells expressing tagged DGK $\eta$  truncation constructs or fluorescent tags alone were washed twice with ice-cold PBS and scraped into ice-cold glycerol coimmunoprecipitation (Co-IP) buffer containing 50 mM HEPES pH 7.4, 250 mM NaCl, 2 mM EDTA, 10% (v/v) glycerol, 0.5% (v/v) BisNonidet P40 substitute, 1× protease inhibitor cocktail, and 1× phosphatase inhibitor cocktail. Cellular debris was removed by centrifugation at 10,000g for 10 minutes at 4°C, and input aliquots of the clarified lysate were set aside. The remaining lysate was then incubated with chicken anti-green fluorescent protein (GFP) primary antibody (Aves Laboratories, Tigard, OR) or normal chicken IgY control (Santa Cruz Biotechnology) for 3 hours at 4°C with gentle mixing. Agarose beads coupled to goat anti-chicken IgY (Aves Laboratories) were then added to each sample and incubated for 1 hour at 4°C. The beads were washed four times (5 minutes/wash) with ice-cold glycerol Co-IP buffer, and bound proteins were eluted from the beads by incubation with 4× Laemmli sample buffer for 15 minutes at 37°C. Input and IP fractions were then separated by SDS-PAGE, transferred to polyvinylidene fluoride membrane, and blotted as described above, using rabbit anti-RFP primary antibody. After imaging, blots were reprobed with rabbit anti-GFP primary antibody (Invitrogen) to determine the specificity of the precipitation. Samples containing RFP alone were heated for 5 minutes at 94°C before SDS-PAGE; samples containing RFP-DGK $\eta$  constructs were not heated, because we found that DGK $\eta$  protein and DGK $\eta$  truncation constructs were undetectable on Western blots when heated at 94°C.

## Results

### Mouse DGK $\eta$ Phosphorylates Multiple DAG Substrates.

First, we set out to evaluate whether mouse DGK $\eta$  isoform 1 was catalytically active (Fig. 1A shows domain structure of isoform 1, henceforth referred to as DGK $\eta$  or DGK $\eta$ 1). To accomplish this, we transfected HEK293 cells with RFP-tagged DGK $\eta$  or RFP only (control) expression constructs. One day later, we prepared cell lysates, incubated these lysates with purified DAG substrates and [ $\gamma$ -<sup>32</sup>P]ATP, then monitored <sup>32</sup>P-labeled phosphatidic acid (<sup>32</sup>P-PA) formation (Fig. 1B). This in vitro assay was previously used to monitor DGK activity (Kanoh et al., 1992; Ohanian and Heagerty, 1994). We found that kinase reactions containing RFP-DGK $\eta$  produced significantly more <sup>32</sup>P-PA than reactions containing RFP alone (Fig. 1C) when 500  $\mu$ M dioctanoyl (8:0), dilauroyl (12:0), or dioleoyl (18:1) glycerol was used as substrate. Given that mouse DGK $\eta$  could phosphorylate multiple DAG substrates, and that 18:1 DAG was previously used to characterize human DGK $\eta$  and other DGK isoforms (Murakami et al., 2003), we elected to use 18:1 DAG for subsequent experiments. Furthermore, we found that 500  $\mu$ M 18:1 DAG was a saturating concentration of substrate (Fig. 1D), justifying our use of this DAG concentration for subsequent in vitro kinase reactions.

### DGK $\eta$ Increases Intracellular Calcium Responses after GPCR Stimulation.

Since DGK $\eta$  is expressed at higher levels in patients with bipolar disorder (Moya et al., 2010), we next sought to determine if overexpression of DGK $\eta$  affects endogenous GPCR signaling. We focused our research on HEK293 cells because they endogenously express the M<sub>3</sub> muscarinic acetylcholine receptor, a G $\alpha_q$ -coupled GPCR that mobilizes intracellular calcium following stimulation with carbachol (Luo et al., 2008). Carbachol causes calcium release by specifically activating the M<sub>3</sub>, but not the M<sub>1</sub>, receptor in HEK293 cells (Luo et al., 2008). Moreover, M<sub>3</sub> receptor

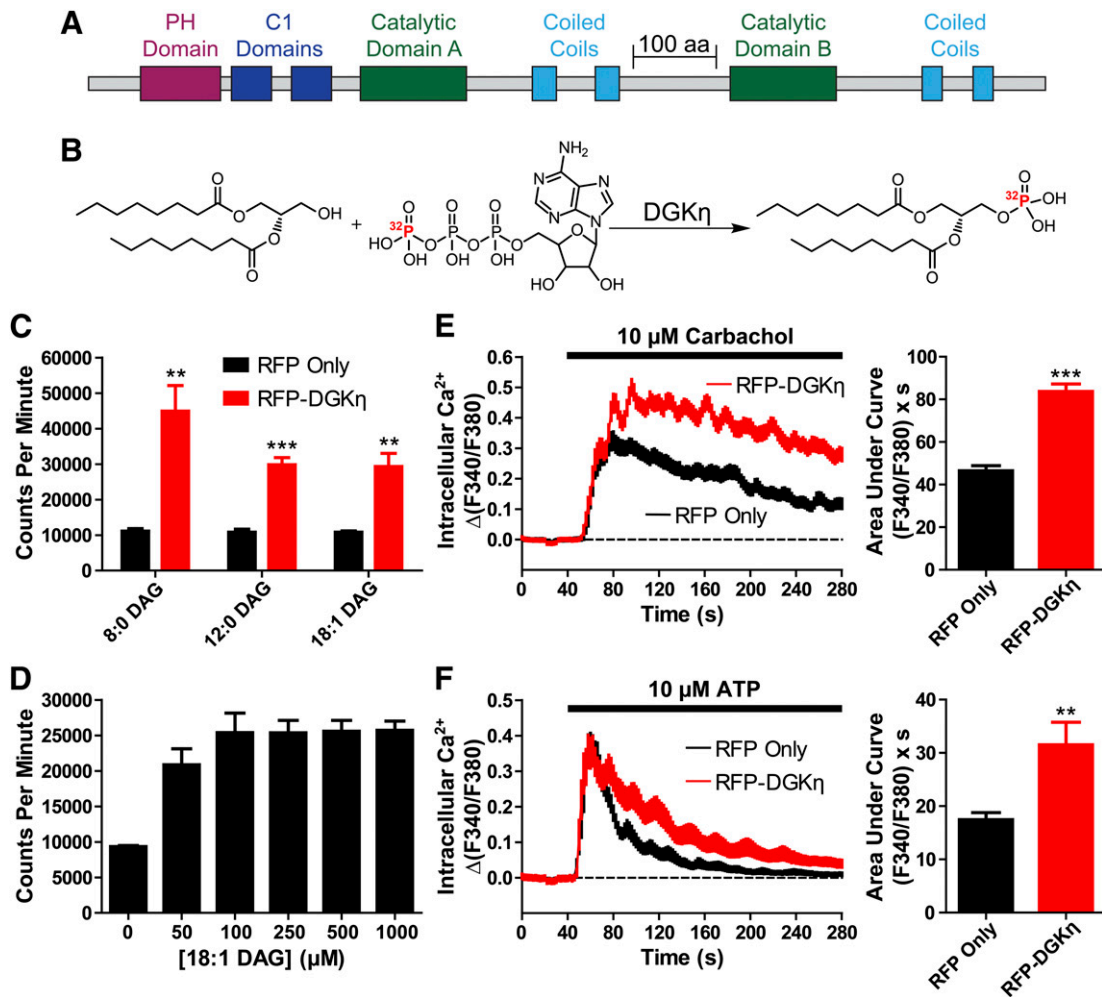


**Fig. 1.** Mouse DGK $\eta$  is catalytically active and enhances GPCR signaling. (A) Domain architecture of DGK $\eta$ . (B) Schematic of the reaction forming  $^{32}\text{P}$ -labeled PA from DAG and radiolabeled ATP. (C) Lysates from HEK293 cells expressing (black) RFP alone or (red) RFP-DGK $\eta$  were incubated with the indicated DAG substrates, each at 500  $\mu\text{M}$ . (D)  $^{32}\text{P}$ -PA production from reactions containing the indicated concentrations of 18:1 DAG, catalyzed by lysates from HEK293 cells expressing RFP-DGK $\eta$ . (E and F) Calcium mobilization in HEK293 cells expressing (black) RFP alone or (red) RFP-DGK $\eta$  after stimulation with (E) 10  $\mu\text{M}$  carbachol or (F) 10  $\mu\text{M}$  ATP. AUC measurements extended for 4 minutes from agonist addition. Data in C and D are the average of two experiments performed in duplicate. Data in E and F are the average of three independent experiments;  $n = 41$ –104 cells per condition. \*\* $P < 0.01$ ; \*\*\* $P < 0.001$  when compared with RFP alone (unpaired  $t$  test). All data, including calcium traces, are presented as means  $\pm$  S.E. C1, PKC homology domain 1; PH, pleckstrin homology.

desensitization and downstream signaling pathways have been extensively studied in HEK293 cells (Rumenapp et al., 2001; Luo et al., 2008). After stimulating with 10  $\mu\text{M}$  carbachol, we found that the calcium mobilization response was enhanced in HEK293 cells expressing RFP-DGK $\eta$  compared with RFP alone (Fig. 1E). Based on quantifying the area under the curve, the carbachol-evoked calcium response in RFP-DGK $\eta$ -expressing cells was 80% greater than in cells expressing RFP alone ( $P < 0.001$ ). However, the peak amplitude of carbachol-evoked calcium responses in cells expressing RFP alone and RFP-DGK $\eta$  was identical (Supplemental Fig. 1), indicating that overexpression of RFP-DGK $\eta$  increases the duration, but not the intensity, of carbachol-evoked calcium mobilization. Indeed, no significant difference in peak amplitudes was observed in the vast majority of calcium mobilization conditions explored in this work (Supplemental Fig. 1), and the few significant differences that were observed were very small and without consistent direction. Furthermore, the N-terminal RFP tag did not affect DGK $\eta$  activity, as untagged

DGK $\eta$ , hemagglutinin-DGK $\eta$ , and DGK $\eta$ -mCherry also enhanced carbachol-evoked calcium responses (data not shown; we identified cells with untagged or hemagglutinin-tagged DGK $\eta$  by cotransfecting with Venus, a yellow fluorescent protein).

We next investigated whether DGK $\eta$  could increase calcium mobilization downstream of other  $G\alpha_q$ -coupled GPCRs. To accomplish this, we stimulated HEK293 cells with 10  $\mu\text{M}$  ATP, which elicits intracellular calcium mobilization by activating endogenous P2Y receptors (Rittiner et al., 2012). We found that HEK293 cells expressing RFP-DGK $\eta$  exhibited elevated ATP-evoked calcium responses compared with cells expressing RFP alone (Fig. 1F). When quantified by AUC, ATP-evoked calcium responses in RFP-DGK $\eta$ -expressing cells were 81% greater than responses in cells expressing RFP alone ( $P < 0.01$ ). These data indicate that overexpression of DGK $\eta$  can enhance calcium responses downstream of two different GPCRs. Since calcium mobilization was more pronounced (longer duration) following endogenous M $_3$  receptor

activation, we focused the remainder of our experiments on DGK $\eta$  modulation of M $_3$  receptor activation.

**DGK $\eta$  Catalytic Activity Is Required to Enhance Carbachol-Evoked Calcium Mobilization.** DGK $\eta$ , like all type 2 DGKs, possesses a split catalytic domain (Sakane et al., 2007). To determine if DGK $\eta$  catalytic activity was required to enhance carbachol-evoked calcium mobilization, we generated two DGK $\eta$  deletion constructs, DGK $\eta$ - $\Delta$ 645 and DGK $\eta$ -646 $\Delta$ , each containing one-half of the catalytic domain (Fig. 2A). We also generated DGK $\eta$ -G389D, containing a point mutation that is predicted to abolish ATP binding based on homology to other DGK proteins (Yamada et al., 2003). We found that DGK $\eta$ - $\Delta$ 645, DGK $\eta$ -646 $\Delta$ , and DGK $\eta$ -G389D were expressed (Supplemental Fig. 2) but were catalytically inactive, as they generated no more  $^{32}$ P-PA than lysates containing RFP alone (Fig. 2B). In contrast, lysates from cells coexpressing DGK $\eta$ - $\Delta$ 645 and DGK $\eta$ -646 $\Delta$  displayed specific activity (catalytic activity normalized for expression; Supplemental Fig. 2) approximately 32% of that of wild-type RFP-DGK $\eta$  (Fig. 2B), suggesting the two halves directly interact. Indeed, we found that RFP-DGK $\eta$ - $\Delta$ 645 coimmunoprecipitated with Venus-DGK $\eta$ -646 $\Delta$  (Fig. 2C). This interaction was specific to DGK $\eta$ - $\Delta$ 645 and DGK $\eta$ -646 $\Delta$  and did not involve the fluorescent tags or nonspecific binding to the immunoprecipitation beads, as evidenced by controls showing no interaction when either construct was replaced with a fluorescent protein alone or when the anti-GFP antibody was replaced with an IgY control (Fig. 2C).

Additionally, none of these catalytically dead constructs (DGK $\eta$ - $\Delta$ 645, DGK $\eta$ -646 $\Delta$ , or DGK $\eta$ -G389D) enhanced calcium mobilization after carbachol stimulation (Fig. 2D). Cells expressing DGK $\eta$ -646 $\Delta$  alone appeared unhealthy and displayed a slight reduction in calcium mobilization. In contrast, coexpression of each half of DGK $\eta$  (RFP-tagged DGK $\eta$ - $\Delta$ 645 and Venus-tagged DGK $\eta$ -646 $\Delta$ ) increased calcium mobilization by 62% (based on AUC measurement, Fig. 2D). These data indicate that DGK $\eta$  catalytic activity is required to enhance carbachol-evoked calcium mobilization.

We next analyzed calcium mobilization AUC data on a cell-by-cell basis, to determine if the expression level of DGK $\eta$  correlated with how effectively DGK $\eta$  enhanced calcium mobilization responses. Notably, there was no relationship between the level of DGK $\eta$  expression and the extent of calcium mobilization in cells expressing WT DGK $\eta$  or kinase-dead DGK $\eta$ -G389D (Fig. 2E). There was also no significant difference in the expression level of WT DGK $\eta$  and DGK $\eta$ -G389D across individual cells. Together, these data suggest that the amount of DGK $\eta$  required to maximally enhance carbachol-evoked calcium mobilization is very small.

We also tested the catalytic activity of several DGK $\eta$  truncation constructs lacking other structural domains (Fig. 3A), again normalized to their expression in HEK293 cells (Supplemental Fig. 2). We found that the pleckstrin homology domain and C-terminal tail negatively regulated DGK $\eta$  catalytic activity, as measured using the *in vitro* kinase assay (Fig. 3B). Truncation of either domain increased DGK $\eta$  specific activity in an additive fashion, and the construct lacking both domains (161 $\Delta$ 961) displayed a specific activity 6-fold higher than WT DGK $\eta$  (Fig. 3B). The C1 domains were required for catalytic activity in this assay, as both constructs lacking C1 domains were inactive (Fig. 3B). Furthermore, the presence of catalytic activity among the DGK $\eta$  truncation constructs correlated with

the ability to enhance carbachol-evoked calcium mobilization (Fig. 3, B and C). However, this correlation was not quantitative. The DGK $\eta$  truncation constructs with greatly increased catalytic activity (compared with WT DGK $\eta$ ) enhanced calcium mobilization to an equal or only marginally increased extent. These data suggest that beyond a certain point, increased DGK $\eta$  catalytic activity does not result in an increased effect upon calcium mobilization. Lastly, we tested the long splice isoform DGK $\eta$ 2, which contains a C-terminal sterile  $\alpha$  motif domain (Fig. 3A), in both the *in vitro* kinase and calcium mobilization assays. We found that DGK $\eta$ 2 had decreased catalytic activity compared with WT DGK $\eta$ 1 (Fig. 3B) as has been reported previously (Murakami et al., 2003), and produced only a negligible ( $P = 0.057$  compared with RFP alone) enhancement of carbachol-evoked calcium mobilization (Fig. 3C). As with WT DGK $\eta$ , we observed no correlation between DGK $\eta$  expression and calcium mobilization for any of the DGK $\eta$  truncation constructs on a cell-by-cell basis (Supplemental Fig. 3).

**DGK $\eta$  Does Not Affect Endoplasmic Reticulum Calcium Loading.** Next, to determine if DGK $\eta$  enhanced calcium responses by affecting the loading of intracellular calcium stores, and not GPCR signaling per se, we treated RFP-DGK $\eta$ -expressing cells and RFP-expressing controls with 1  $\mu$ M thapsigargin in the presence of extracellular calcium. Thapsigargin is a noncompetitive sarco/endoplasmic reticulum calcium ATPase inhibitor that causes the release of intracellular calcium store contents into the cytosol (Jackson et al., 1988). Calcium release was not significantly different between cells expressing RFP alone and RFP-DGK $\eta$  (Fig. 4A), indicating that DGK $\eta$  has no effect on the loading of intracellular calcium stores.

When intracellular calcium stores become depleted, calcium-sensing proteins trigger the opening of calcium channels in the plasma membrane, allowing the entry of extracellular calcium, a process known as store-operated calcium entry (Venkatachalam et al., 2002). To determine if DGK $\eta$  enhanced calcium mobilization by affecting this process, we stimulated cells with carbachol in the absence of extracellular calcium (to abolish calcium entry through any channels or transporters). In the absence of extracellular calcium, carbachol-evoked calcium mobilization was reduced, particularly in the later stages of the response (compare Fig. 4B with Fig. 1E). However, overexpression of DGK $\eta$  still enhanced the calcium response by 77% (based on AUC measurements) when compared with RFP alone. This effect was nearly identical to the 80% AUC increase in the presence of extracellular calcium (Fig. 1E). Thus, these data indicate that DGK $\eta$  enhances the carbachol-evoked calcium response via a mechanism that is not solely dependent upon the modulation of calcium entry.

**DGK $\eta$  Does Not Translocate after GPCR Stimulation.** Human DGK $\eta$  localizes to the cytosol under baseline conditions and translocates to endosomes after osmotic shock (Murakami et al., 2003; Matsutomo et al., 2013). However, whether DGK $\eta$  translocates to the plasma membrane or intracellular compartments following GPCR stimulation is unknown. Using live cell confocal imaging, we found that mouse DGK $\eta$  is localized throughout the cytoplasm in unstimulated cells and did not translocate to the plasma membrane or to any intracellular compartment after stimulating with 10  $\mu$ M carbachol at room temperature (Fig. 5A). This experiment was conducted under conditions that were identical to those used in the carbachol-evoked calcium mobilization assay, suggesting that the effects of

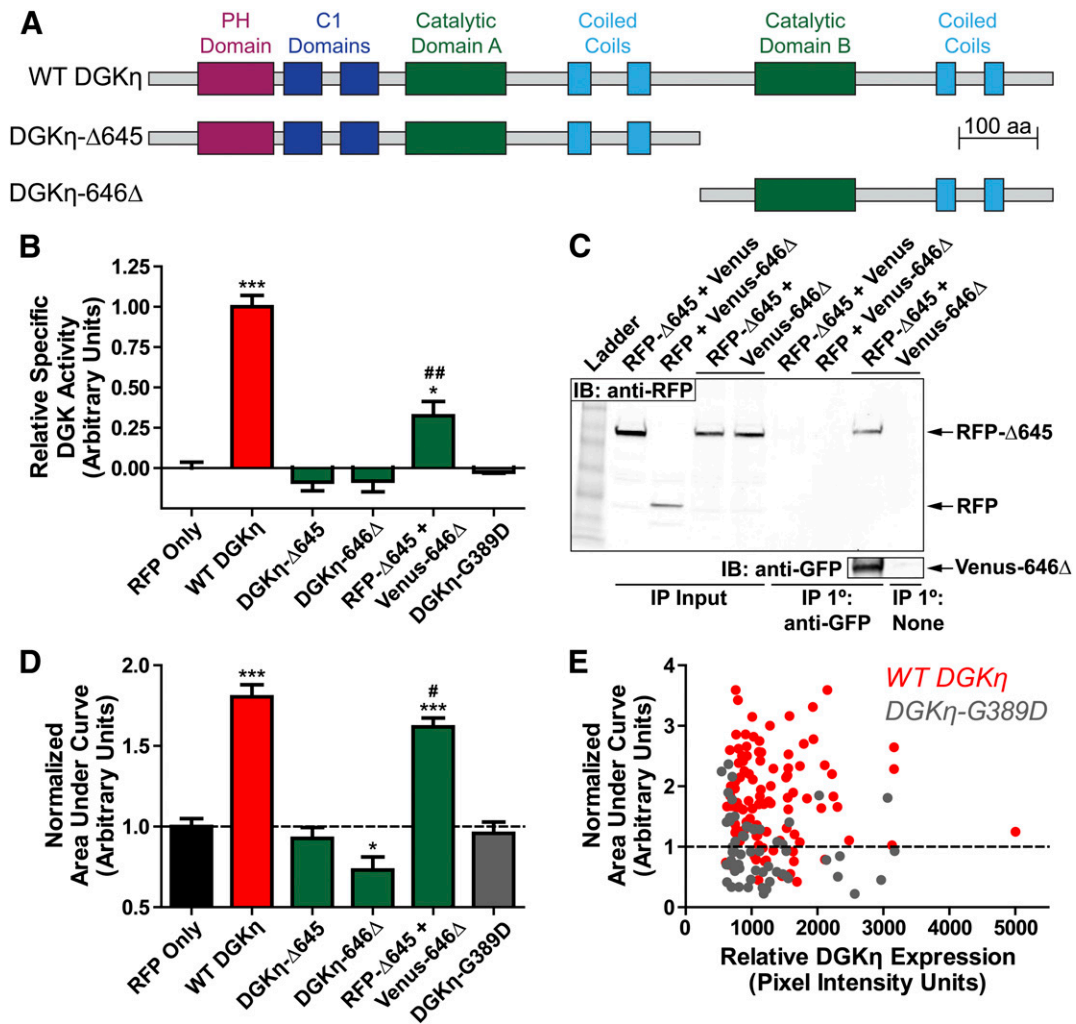


**Fig. 2.** DGK $\eta$  catalytic activity is required to enhance GPCR signaling. (A) Structure of the DGK $\eta$  constructs used. DGK $\eta$ -G389D contains a point mutation in catalytic domain A. All DGK $\eta$  constructs were N-terminally tagged with RFP unless otherwise noted. (B) Production of  $^{32}$ P-PA in reactions containing the indicated DGK $\eta$  constructs, using 500  $\mu$ M 18:1 DAG as substrate. Data were normalized to DGK $\eta$  expression, which was assessed by Western blotting against RFP, then normalized so that RFP alone = 0 and WT DGK $\eta$  = 1. Data are the average of two experiments performed in duplicate. (C) Lysates from HEK293 cells expressing RFP-tagged DGK $\eta$ - $\Delta$ 645 and Venus-tagged DGK $\eta$ -646 $\Delta$  or fluorescent protein controls were immunoprecipitated using an anti-GFP antibody or an IgY control. Input and precipitated fractions were then run on SDS-PAGE and blotted using an anti-RFP antibody. The blot was later reprobbed with an anti-GFP antibody to verify the specificity of the immunoprecipitation. (D) AUC measurements of calcium mobilization in HEK293 cells expressing the indicated DGK $\eta$  constructs after stimulation with 10  $\mu$ M carbachol, normalized such that RFP alone = 1. AUC data for the RFP and WT DGK $\eta$  conditions are also presented, in non-normalized form, in Fig. 1E. Data are the average of three to six independent experiments;  $n$  = 58–162 cells per condition, except DGK $\eta$ -646 $\Delta$ , where  $n$  = 23. (E) Scatter plot comparing calcium mobilization AUC measurements to DGK $\eta$  expression levels in individual HEK293 cells expressing (red) WT DGK $\eta$  or (gray) DGK $\eta$ -G389D. Horizontal dashed line indicates average level of calcium mobilization in HEK293 cells expressing RFP alone. \* $P$  < 0.05; \*\*\* $P$  < 0.001 when compared with RFP alone. # $P$  < 0.05; ## $P$  < 0.01 when compared with WT DGK $\eta$ . Unpaired  $t$  tests were used to compare data. All data are presented as means  $\pm$  S.E.

DGK $\eta$  on GPCR signaling require little if any translocation of DGK $\eta$ . Furthermore, we were unable to detect translocation of DGK $\eta$  when cells were stimulated with 10 or 100  $\mu$ M carbachol at 37 $^\circ$ C (data not shown). Our inability to detect DGK $\eta$  translocation was not a technical limitation, as our mouse DGK $\eta$  construct rapidly translocated to endosomes after osmotic shock at room temperature (Fig. 5B), as previously shown using human DGK $\eta$  (Murakami et al., 2003; Matsutomo et al., 2013).

**DGK $\eta$  Enhances GPCR Signaling by Attenuating PKC Activation.** DAG is a canonical activator of conventional and novel isoforms of PKC (Mellor and Parker, 1998). Additionally, PKC is directly and indirectly involved in the phosphorylation and subsequent desensitization of GPCRs (Krasel et al., 2001; Kelly et al., 2008; Feng et al., 2011).

Therefore, we hypothesized that DGK $\eta$  might enhance GPCR signaling by metabolizing DAG and hence reducing PKC activation. First, we confirmed that acute treatment with 300-nM PMA could activate PKC in HEK293 cells. PMA is a phorbol ester that is structurally similar to DAG and potentially activates multiple PKC isoforms (Blumberg, 1988). For this control experiment, we focused on PKC $\delta$  because it is highly expressed in HEK293 cells (Leaney et al., 2001) and it is a Ca $^{2+}$ -insensitive isoform of PKC (Mellor and Parker, 1998). We found that PMA induced a rapid (within 2 minutes) translocation of PKC $\delta$  to the plasma membrane (Fig. 6A). However, 300 nM PMA did not induce translocation of overexpressed RFP-DGK $\eta$  to the plasma membrane or any other cellular compartment during the same time frame (data not shown). We then measured calcium mobilization after

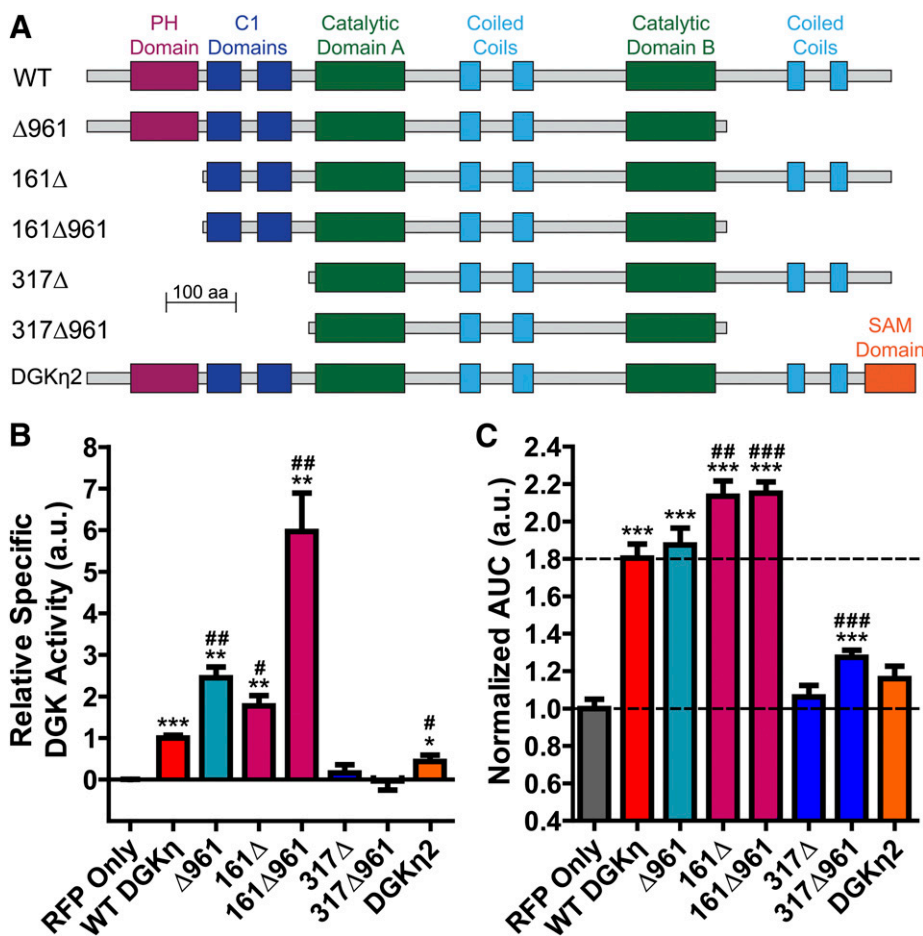


**Fig. 3.** Catalytic activity and signaling effects of additional DGK $\eta$  truncation constructs. (A) Domain architecture of the indicated DGK $\eta$  constructs. All constructs were N-terminally tagged with RFP. (B) Production of  $^{32}\text{P}$ -PA in reactions with the indicated DGK $\eta$  constructs, using 500  $\mu\text{M}$  18:1 DAG as substrate. Data were normalized to DGK $\eta$  expression, which was assessed by Western blotting against RFP, then normalized so that RFP alone = 0 and WT DGK $\eta$  = 1. Data are the average of two experiments performed in duplicate. (C) AUC measurements of calcium mobilization in HEK293 cells expressing the indicated DGK $\eta$  constructs after stimulation with 10  $\mu\text{M}$  carbachol, normalized such that RFP alone = 1. Data are the average of three to six independent experiments;  $n = 75$ –209 cells per condition. \* $P < 0.05$ ; \*\* $P < 0.01$ ; \*\*\* $P < 0.001$  when compared with RFP alone. # $P < 0.05$ ; ## $P < 0.01$ ; ### $P < 0.001$  when compared with WT DGK $\eta$ . Unpaired  $t$  tests were used to compare data. All data are presented as means  $\pm$  S.E.

stimulating RFP- and RFP-DGK $\eta$ -expressing cells with 300 nM PMA followed immediately by 10  $\mu\text{M}$  carbachol. Stimulation with 300 nM PMA profoundly accelerated the return of carbachol-evoked calcium mobilization to baseline (compare Fig. 6B with Fig. 1E). Furthermore, the carbachol-evoked calcium responses were identical in cells expressing RFP alone and RFP-DGK $\eta$  when PKC was acutely activated with 300 nM PMA (Fig. 6B). In contrast, stimulation of RFP-expressing cells with 300 nM PMA alone did not evoke a calcium response (Fig. 6B). Taken together, these data indicate that PKC activation blunts GPCR signaling in HEK293 cells and occludes the effect of DGK $\eta$ .

We next determined whether pharmacological inhibition of PKC activity would enhance GPCR signaling, using the cell-permeable PKC inhibitor bisindolylmaleimide I (Toullec et al., 1991). We found that carbachol-evoked calcium mobilization in RFP-expressing HEK293 cells was dramatically enhanced after preincubation with 1  $\mu\text{M}$  BIM I (Fig. 6C). This effect was nearly identical to that observed after expression of RFP-DGK $\eta$  (compare Fig. 6C with Fig. 1E). Indeed, BIM I pretreatment yielded an 81% increase in calcium responses (based on AUC measurements), essentially the same as the 80% AUC increase observed after RFP-DGK $\eta$  expression (Fig. 1E). Furthermore, carbachol-evoked calcium responses were indistinguishable in RFP- and RFP-DGK $\eta$ -expressing cells after pretreatment with BIM I (Fig. 6C). A different PKC inhibitor (1  $\mu\text{M}$  Gö6976) also enhanced calcium mobilization to nearly the same extent in RFP-expressing and

RFP-DGK $\eta$ -expressing cells (Fig. 6D), although the kinetics were different when compared with BIM I, possibly because Gö6976 is selective for the  $\text{Ca}^{2+}$ -sensitive PKC $\alpha$  and PKC $\beta$  isoforms (Martiny-Baron et al., 1993). Taken together, these data show that pharmacological inhibition of PKC activity both mimics the effect of DGK $\eta$  and prevents overexpressed DGK $\eta$  from enhancing calcium mobilization further. The latter finding suggests that PKC inhibitors and overexpressed DGK $\eta$  work via a similar mechanism—by inhibiting PKC directly (inhibitors) or indirectly (by depleting the PKC activator DAG). Thus, these data suggest that DGK $\eta$  potentiates GPCR signaling via PKC, likely by reducing the levels of a PKC activator (DAG) and attenuating PKC activity.

## Discussion

Collectively, our data suggest a model for how DGK $\eta$  enhances GPCR signaling (Fig. 7). Stimulation of  $\text{G}\alpha_q$ -coupled GPCRs leads to the activation of phospholipase C and the hydrolysis of phosphatidylinositol 4,5-bisphosphate into inositol 1,4,5-trisphosphate and DAG. Inositol 1,4,5-trisphosphate subsequently induces the release of calcium from endoplasmic reticulum calcium stores, raising the cytosolic concentration of  $\text{Ca}^{2+}$ . In cells not overexpressing DGK $\eta$  (Fig. 7A), DAG activates PKC, leading to the phosphorylation and desensitization of the activated GPCR, followed by termination of GPCR signaling (Tang et al., 1995; Gereau and Heinemann, 1998; Kelly et al., 2008). However, in cells overexpressing DGK $\eta$ ,

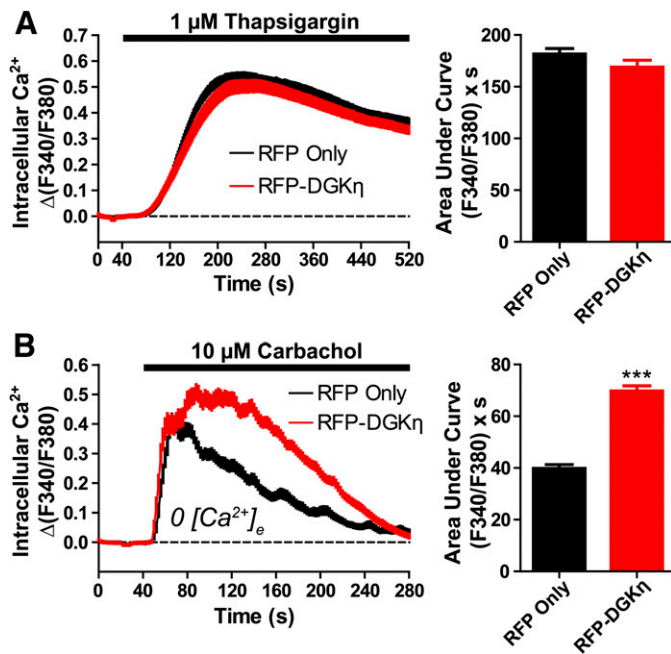


**Fig. 4.** DGK $\eta$  does not affect intracellular calcium stores. Calcium mobilization in HEK293 cells expressing (black) RFP alone or (red) RFP-DGK $\eta$  after (A) stimulation with 1  $\mu\text{M}$  thapsigargin or (B) stimulation with 10  $\mu\text{M}$  carbachol in the absence of extracellular calcium. AUC measurements extended 8 minutes (A) or 4 minutes (B) after stimulation. Data are the average of two (A) or five (B) independent experiments;  $n = 69$ –190 cells per condition. \*\*\* $P < 0.001$  when compared with RFP alone (unpaired  $t$  test). All data, including calcium traces, are presented as means  $\pm$  S.E.

DAG is phosphorylated to PA, leading to a decreased level of PKC activation (Fig. 7B, red). This causes a decrease in the rate of GPCR phosphorylation and desensitization, resulting in enhanced GPCR signaling (as evidenced by elevated intracellular calcium release).

During activation, PKC isoforms translocate to the plasma membrane (Nishizuka, 1984), and are autophosphorylated at multiple amino acid residues (Keränen et al., 1995; Newton, 2003). We attempted to measure PKC activation directly via: 1) PKC $\delta$  immunostaining (Fig. 6A), 2) membrane/cytosol fractionation and PKC $\delta$  Western blotting (Brown et al., 2005), 3) anti-phospho-PKC $\delta$  Western blotting (Sumandea et al., 2008), 4) anti-pan-phospho-PKC Western blotting (Iwabu et al., 2004), 5) a GFP biosensor based on the C1 domains of PKC $\gamma$  (Oancea et al., 1998), and 6) a FRET biosensor of PKC activity (Violin et al., 2003). Unfortunately, we did not observe endogenous PKC activation with any of these techniques after stimulating endogenous M $_3$  receptors with carbachol, and were therefore unable to directly measure the effect of DGK $\eta$  on endogenous PKC activity. This did not reflect technical limitations, as we did observe endogenous PKC $\delta$  activation after direct stimulation with PMA (Fig. 6A). Instead, our inability to directly measure endogenous PKC activity suggests very little PKC is activated when endogenous receptors are stimulated, likely due to a low level of DAG release. Indeed, we observed that only a minimal level of DGK $\eta$  expression results in the full enhancing effect on calcium mobilization (Fig. 2E), and that increased DGK $\eta$  catalytic activity does not increase this effect beyond a certain point (Fig. 3C). Both these observations are entirely consistent with DGK $\eta$  activity being

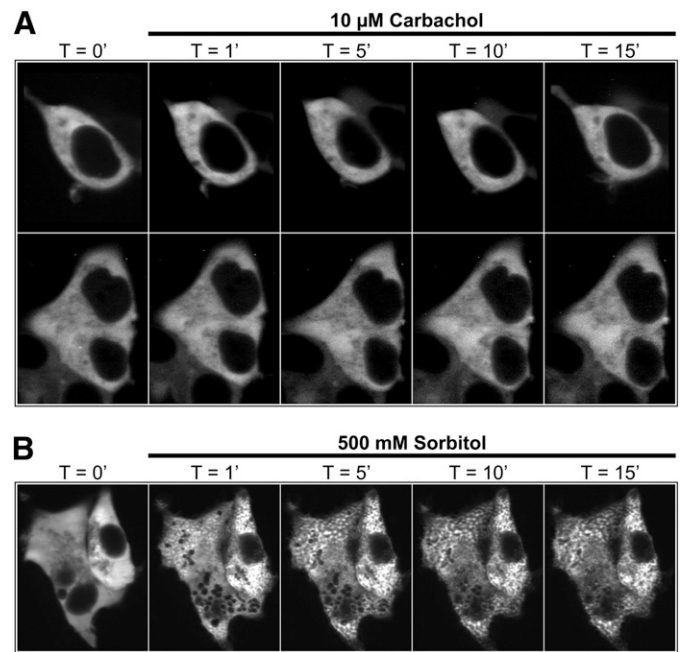


**Fig. 5.** DGK $\eta$  does not translocate within cells after GPCR stimulation. Confocal images of live HEK293 cells expressing RFP-DGK $\eta$  after stimulation with (A) 10  $\mu\text{M}$  carbachol or (B) 500 mM sorbitol for the indicated times. Cell culture and imaging conditions were identical to those used in calcium mobilization experiments. (A) Cells from independent experiments are shown in each row.

constrained by a low level of available DAG substrate. In further support of this possibility, we did not detect an increase in DAG levels after activating the endogenous M $_3$  receptor with carbachol (using a sensitive DAG biosensor, Upward DAG2; data not shown) (Tewson et al., 2013).

Previous studies that measured PKC activity employed overexpressed receptors (Iwabu et al., 2004; Brown et al., 2005). It is well documented that overexpressed receptors activate signaling pathways at nonphysiologic (excessive) levels relative to endogenous receptor activation (Dickson et al., 2013). This is precisely why we used endogenous M $_3$  receptors and a sub-EC $_{50}$  concentration of carbachol (Luo et al., 2008) in our signaling experiments to probe potential negative and positive modulation at physiologic levels of GPCR activation. Although we were unable to directly measure changes in endogenous PKC activity when stimulating with carbachol, modulation of PKC activity clearly mediates the effect of DGK $\eta$  on GPCR signaling, as both activation (Fig. 6B) and inhibition (Fig. 6C) of PKC blocked overexpressed DGK $\eta$  from enhancing endogenous M $_3$  receptor activation.

It is well established that PKC activation leads to desensitization of GPCRs (Tang et al., 1995; Gereau and Heinemann, 1998; Kelly et al., 2008). Based on this literature, we suggest that overexpression of DGK $\eta$  enhances GPCR signaling by attenuating PKC-mediated phosphorylation and desensitization of GPCRs (Fig. 7). Such a mechanism should have a greater effect on the duration of calcium responses than the intensity, consistent with our findings (Fig. 1, E and F; Supplemental Fig. 1). Likewise, cholinergic stimulation of cells expressing a phosphorylation-deficient M $_3$  receptor resulted in enhanced calcium mobilization when compared with cells expressing wild-type M $_3$  receptor (Kong et al., 2010), resembling the effect of



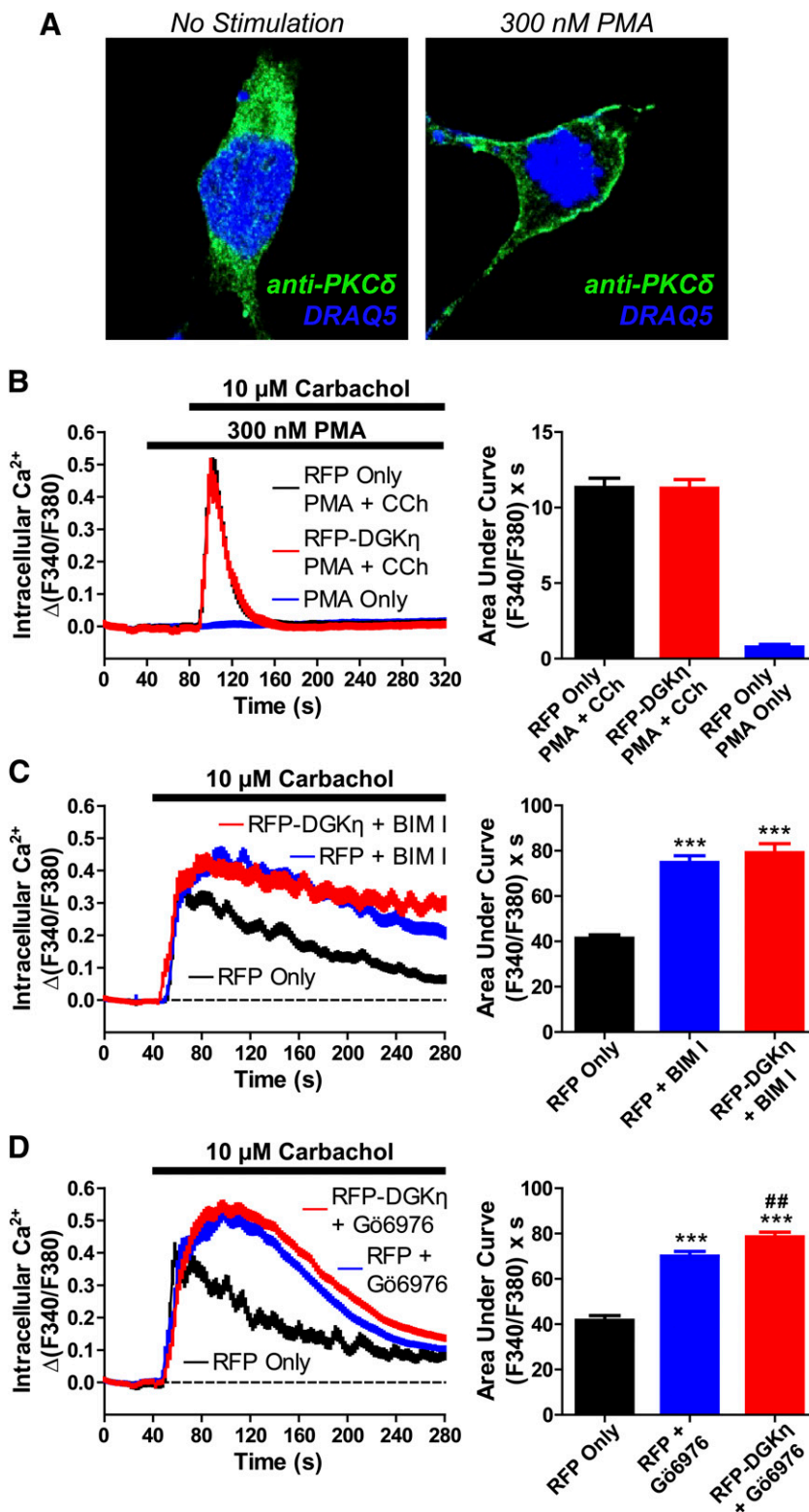


**Fig. 6.** DGK $\eta$  enhances GPCR signaling via PKC. (A) PKC $\delta$  translocation following PMA stimulation. Confocal images of HEK293 cells after treatment with (left) vehicle or (right) 300 nM PMA for 2 minutes. Cells were fixed, immunostained with an anti-PKC $\delta$  antibody (green), and counterstained with DRAQ5 nuclear dye (blue). (B) Calcium mobilization in HEK293 cells expressing (black, blue) RFP alone or (red) RFP-DGK $\eta$  after stimulation with (black, red) 300 nM PMA followed by 10  $\mu$ M carbachol, or (blue) 300 nM PMA alone. AUC measurements extended 80 seconds from final agonist addition. Data are the average of two (PMA alone) or three (PMA + carbachol) independent experiments;  $n = 49-83$  cells per condition. (C and D) Calcium mobilization in HEK293 cells expressing (black, blue) RFP alone or (red) RFP-DGK $\eta$  after pretreatment with (blue, red) 1  $\mu$ M PKC inhibitor (C) BIM I or (D) Gö6976. Cells were stimulated with 10  $\mu$ M carbachol, and AUC measurements extended 4 minutes from agonist addition. Data in C are the average of five independent experiments;  $n = 140-198$  cells per condition. Data in D are the average of three independent experiments;  $n = 85-148$  cells per condition. \*\*\* $P < 0.001$  when compared with RFP in the absence of PKC inhibitor; ## $P < 0.01$  when compared with RFP plus Gö6976. Unpaired  $t$  tests were used to compare data. All data, including calcium traces, are presented as means  $\pm$  S.E.

overexpressed DGK $\eta$  following M $_3$  receptor activation. However, it remains possible that another mechanism downstream of PKC, such as modulation of calcium transporter activity (Usachev et al., 2002, 2006), is responsible for the increased duration of calcium responses observed in DGK $\eta$ -expressing cells.

Note that M $_3$  receptor internalization (as distinct from desensitization) is not likely to be involved in DGK $\eta$ -mediated modulation of receptor signaling, as internalization of the M $_3$  receptor is very slow (hours), even during continuous stimulation with an extremely high concentration of carbachol (Thangaraju and Sawyer, 2011). Although PKC directly

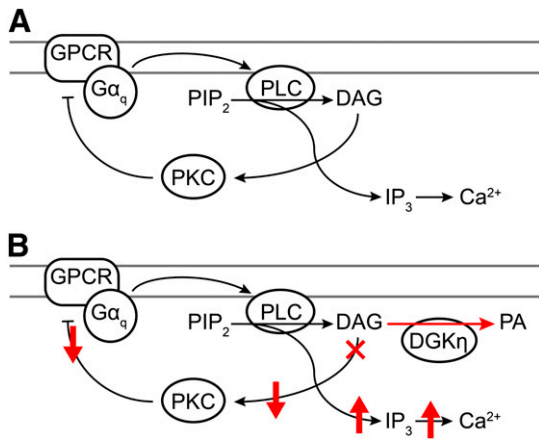


**Fig. 7.** Model showing how DGK $\eta$  enhances G $\alpha_q$ -coupled GPCR signaling. (A) Activation of G $\alpha_q$ -coupled GPCRs leads to the stimulation of phospholipase C (PLC)-catalyzed hydrolysis of phosphatidylinositol 4,5-bisphosphate (PIP<sub>2</sub>) and the release of inositol 1,4,5-trisphosphate (IP<sub>3</sub>) and DAG. IP<sub>3</sub> activates IP<sub>3</sub> receptors on the endoplasmic reticulum, resulting in the release of calcium from intracellular calcium stores. Concurrently, DAG activates conventional and novel isoforms of PKC, leading to the phosphorylation of activated GPCRs, resulting in receptor desensitization and the attenuation of GPCR signaling. (B) After receptor activation, overexpressed DGK $\eta$  reduces the pool of free DAG by converting it into PA, thus suppressing the activation of PKC. As described in the literature (see *Discussion*), reduced PKC activity attenuates GPCR desensitization. This leads to enhanced IP<sub>3</sub> and intracellular calcium release following receptor activation.

phosphorylates some GPCRs (Kelly et al., 2008; Feng et al., 2011), phosphorylation of the M<sub>3</sub> receptor in HEK293 cells could be indirect, through the activation of G protein-coupled receptor kinases. In HEK293 cells, M<sub>3</sub> receptor activity is regulated by GRKs 2, 3, and 6 (Luo et al., 2008), at least one of which is activated by PKC (Krasel et al., 2001). Interestingly, GRK3 is also genetically linked to BPD (Rao et al., 2009), suggesting that dysregulation of GPCR signaling is important in the pathology of BPD.

Other DGK isoforms regulate PKC and receptor signaling. For example, disruption of the gene encoding DGK $\delta$  leads to DAG accumulation and enhanced PKC activity and epidermal growth factor receptor (EGFR) phosphorylation (Crotty et al., 2006), culminating in a PKC-dependent increase in EGFR ubiquitination and degradation (Cai et al., 2010). DGKs also regulate inter-receptor desensitization pathways, as DGK $\theta$  attenuates bradykinin-evoked, PKC-mediated phosphorylation of EGFR, a phosphorylation event that is linked to EGFR desensitization (van Baal et al., 2012). Interestingly, EGFR is a receptor tyrosine kinase, indicating that regulation of receptor signaling by DGKs is not limited to GPCRs. These studies, when combined with our current study, suggest that multiple members of the DGK enzyme family can regulate PKC activity and receptor signaling.

Lastly, our study provides new insights into how alterations in DGK $\eta$  might affect cellular signaling in patients with BPD. Numerous genome-wide association studies have linked single nucleotide polymorphisms within *DGKH* to BPD (Baum et al., 2008; Squassina et al., 2009; Takata et al., 2011; Weber et al., 2011; Yosifova et al., 2011; Zeng et al., 2011), although whether these single nucleotide polymorphisms increase, decrease, or have no effect on *DGKH* expression is unknown. In one study, *DGKH* was found to be expressed at higher levels in postmortem tissues from

patients with BPD than unaffected controls (Moya et al., 2010), suggesting that DGK $\eta$  enzymatic activity might also be elevated. Given that overexpression of DGK $\eta$  enhanced GPCR signaling in a model cell line, it is tempting to speculate that GPCR signaling might be dysregulated in other cell types when DGK $\eta$  activity is increased or decreased. Ultimately, future studies will be needed to delineate precisely how DGK $\eta$  activity is altered in BPD patients and how such alterations affect PKC and GPCR signaling in neurons and in animal models of BPD.

#### Acknowledgments

The authors thank Joyce Ohiri and Suzanne Nobles for conducting pilot experiments, and Montana Molecular for the fluorescent DAG biosensor construct.

#### Authorship Contributions

*Participated in research design:* Rittiner, Zylka.

*Conducted experiments:* Rittiner, Brings.

*Performed data analysis:* Rittiner.

*Wrote or contributed to the writing of the manuscript:* Rittiner, Brings, Zylka.

#### References

- Avissar S, Schreiber G, Danon A, and Belmaker RH (1988) Lithium inhibits adrenergic and cholinergic increases in GTP binding in rat cortex. *Nature* **331**:440–442.
- Baum AE, Akula N, Cabanero M, Cardona I, Corona W, Klemens B, Schulze TG, Cichon S, Rietschel M, and Nöthen MM et al. (2008) A genome-wide association study implicates diacylglycerol kinase eta (DGKH) and several other genes in the etiology of bipolar disorder. *Mol Psychiatry* **13**:197–207.
- Blumberg PM (1988) Protein kinase C as the receptor for the phorbol ester tumor promoters: sixth Rhoads memorial award lecture. *Cancer Res* **48**:1–8.
- Brown SG, Thomas A, Dekker LV, Tinker A, and Leaney JL (2005) PKC-delta sensitizes Kir3.1/3.2 channels to changes in membrane phospholipid levels after M3 receptor activation in HEK-293 cells. *Am J Physiol Cell Physiol* **289**:C543–C556.
- Cai J, Crotty TM, Reichert E, Carraway KL, 3rd, Stafforini DM, and Topham MK (2010) Diacylglycerol kinase delta and protein kinase C(alpha) modulate epidermal growth factor receptor abundance and degradation through ubiquitin-specific protease 8. *J Biol Chem* **285**:6952–6959.
- Catapano LA and Manji HK (2007) G protein-coupled receptors in major psychiatric disorders. *Biochim Biophys Acta* **1768**:976–993.
- Crotty T, Cai J, Sakane F, Taketomi A, Prescott SM, and Topham MK (2006) Diacylglycerol kinase delta regulates protein kinase C and epidermal growth factor receptor signaling. *Proc Natl Acad Sci USA* **103**:15485–15490.
- Dickson EJ, Falkenburger BH, and Hille B (2013) Quantitative properties and receptor reserve of the IP(3) and calcium branch of G(q)-coupled receptor signaling. *J Gen Physiol* **141**:521–535.
- Feng B, Li Z, and Wang JB (2011) Protein kinase C-mediated phosphorylation of the  $\mu$ -opioid receptor and its effects on receptor signaling. *Mol Pharmacol* **79**:768–775.
- Friedman E and Wang HY (1996) Receptor-mediated activation of G proteins is increased in postmortem brains of bipolar affective disorder subjects. *J Neurochem* **67**:1145–1152.
- Gereau RW, 4th and Heinemann SF (1998) Role of protein kinase C phosphorylation in rapid desensitization of metabotropic glutamate receptor 5. *Neuron* **20**:143–151.
- Gregg LC, Jung KM, Spradley JM, Nylas R, Suplita RL, 2nd, Zimmer A, Watanabe M, Mackie K, Katona I, and Piomelli D et al. (2012) Activation of type 5 metabotropic glutamate receptors and diacylglycerol lipase- $\alpha$  initiates 2-arachidonoylglycerol formation and endocannabinoid-mediated analgesia. *J Neurosci* **32**:9457–9468.
- Hahn CG, Umapathy, Wang HY, Koneru R, Levinson DF, and Friedman E (2005) Lithium and valproic acid treatments reduce PKC activation and receptor-G protein coupling in platelets of bipolar manic patients. *J Psychiatr Res* **39**:355–363.
- Iwabu A, Smith K, Allen FD, Lauffenburger DA, and Wells A (2004) Epidermal growth factor induces fibroblast contractility and motility via a protein kinase C delta-dependent pathway. *J Biol Chem* **279**:14551–14560.
- Jackson TR, Patterson SI, Thastrup O, and Hanley MR (1988) A novel tumour promoter, thapsigargin, transiently increases cytoplasmic free Ca<sup>2+</sup> without generation of inositol phosphates in NG115-401L neuronal cells. *Biochem J* **253**:81–86.
- Jenkins GH, Fisetite PL, and Anderson RA (1994) Type I phosphatidylinositol 4-phosphate 5-kinase isoforms are specifically stimulated by phosphatidic acid. *J Biol Chem* **269**:11547–11554.
- Kanoh H, Sakane F, and Yamada K (1992) Diacylglycerol kinase isozymes from brain and lymphoid tissues. *Methods Enzymol* **209**:162–172.
- Kelly E, Bailey CP, and Henderson G (2008) Agonist-selective mechanisms of GPCR desensitization. *Br J Pharmacol* **153** (Suppl 1):S379–S388.
- Keranen LM, Dutil EM, and Newton AC (1995) Protein kinase C is regulated in vivo by three functionally distinct phosphorylations. *Curr Biol* **5**:1394–1403.
- Klauck TM, Xu X, Mousseau B, and Jaken S (1996) Cloning and characterization of a glucocorticoid-induced diacylglycerol kinase. *J Biol Chem* **271**:19781–19788.
- Kong KC, Butcher AJ, McWilliams P, Jones D, Wess J, Hamdan FF, Werry T, Rosethorne EM, Charlton SJ, and Munson SE et al. (2010) M3-muscarinic receptor

- promotes insulin release via receptor phosphorylation/arrestin-dependent activation of protein kinase D1. *Proc Natl Acad Sci USA* **107**:21181–21186.
- Krasel C, Dammeier S, Winstel R, Brockmann J, Mischak H, and Lohse MJ (2001) Phosphorylation of GRK2 by protein kinase C abolishes its inhibition by calmodulin. *J Biol Chem* **276**:1911–1915.
- Leaney JL, Dekker LV, and Tinker A (2001) Regulation of a G protein-gated inwardly rectifying K<sup>+</sup> channel by a Ca(2<sup>+</sup>)-independent protein kinase C. *J Physiol* **534**:367–379.
- Lucas P, Ukhanov K, Leinders-Zufall T, and Zufall F (2003) A diacylglycerol-gated cation channel in vomeronasal neuron dendrites is impaired in TRPC2 mutant mice: mechanism of pheromone transduction. *Neuron* **40**:551–561.
- Luo J, Busillo JM, and Benovic JL (2008) M3 muscarinic acetylcholine receptor-mediated signaling is regulated by distinct mechanisms. *Mol Pharmacol* **74**:338–347.
- Martiny-Baron G, Kazanietz MG, Mischak H, Blumberg PM, Kochs G, Hug H, Marmé D, and Schächtele C (1993) Selective inhibition of protein kinase C isozymes by the indolocarbazole Gö 6976. *J Biol Chem* **268**:9194–9197.
- Matsutomo D, Isozaki T, Sakai H, and Sakane F (2013) Osmotic shock-dependent redistribution of diacylglycerol kinase  $\eta$ 1 to non-ionic detergent-resistant membrane via pleckstrin homology and C1 domains. *J Biochem* **153**:179–190.
- Mellor H and Parker PJ (1998) The extended protein kinase C superfamily. *Biochem J* **332**:281–292.
- Mérida I, Avila-Flores A, and Merino E (2008) Diacylglycerol kinases: at the hub of cell signalling. *Biochem J* **409**:1–18.
- Moya PR, Murphy DL, McMahon FJ, and Wendland JR (2010) Increased gene expression of diacylglycerol kinase  $\eta$  in bipolar disorder. *Int J Neuropsychopharmacol* **13**:1127–1128.
- Murakami T, Sakane F, Imai S, Houkin K, and Kanoh H (2003) Identification and characterization of two splice variants of human diacylglycerol kinase  $\eta$ . *J Biol Chem* **278**:34364–34372.
- Nakano T, Iravani A, Kim M, Hozumi Y, Lohse M, Reichert E, Crotty TM, Stafforini DM, and Topham MK (2014) Diacylglycerol kinase  $\eta$  modulates oncogenic properties of lung cancer cells. *Clin Transl Oncol* **16**:29–35.
- Newton AC (2003) Regulation of the ABC kinases by phosphorylation: protein kinase C as a paradigm. *Biochem J* **370**:361–371.
- Nishizuka Y (1984) The role of protein kinase C in cell surface signal transduction and tumour promotion. *Nature* **308**:693–698.
- Oancea E, Teruel MN, Quest AF, and Meyer T (1998) Green fluorescent protein (GFP)-tagged cysteine-rich domains from protein kinase C as fluorescent indicators for diacylglycerol signaling in living cells. *J Cell Biol* **140**:485–498.
- Ohanian J and Heagerty AM (1994) Membrane-associated diacylglycerol kinase activity is increased by noradrenaline, but not by angiotensin II, in arterial smooth muscle. *Biochem J* **300**:51–56.
- Pantazopoulos H, Stone D, Walsh J, and Benes FM (2004) Differences in the cellular distribution of D1 receptor mRNA in the hippocampus of bipolars and schizophrenics. *Synapse* **54**:147–155.
- Rao JS, Rapoport SI, and Kim HW (2009) Decreased GRK3 but not GRK2 expression in frontal cortex from bipolar disorder patients. *Int J Neuropsychopharmacol* **12**:851–860.
- Rittiner JE, Korboukh I, Hull-Ryde EA, Jin J, Janzen WP, Frye SV, and Zylka MJ (2012) AMP is an adenosine A1 receptor agonist. *J Biol Chem* **287**:5301–5309.
- Rümenapp U, Asmus M, Schabrowski H, Woznicki M, Han L, Jakobs KH, Fahimi-Vahid M, Michalek C, Wieland T, and Schmidt M (2001) The M3 muscarinic acetylcholine receptor expressed in HEK-293 cells signals to phospholipase D via G12 but not Gq-type G proteins: regulators of G proteins as tools to dissect pertussis toxin-resistant G proteins in receptor-effector coupling. *J Biol Chem* **276**:2474–2479.
- Sakane F, Imai S, Kai M, Yasuda S, and Kanoh H (2007) Diacylglycerol kinases: why so many of them? *Biochim Biophys Acta* **1771**:793–806.
- Squassina A, Manchia M, Congiu D, Severino G, Chillotti C, Ardu R, Piccardi M, and Zompo MD (2009) The diacylglycerol kinase  $\eta$  gene and bipolar disorder: a replication study in a Sardinian sample. *Mol Psychiatry* **14**:350–351.
- Sumandea MP, Rybin VO, Hinken AC, Wang C, Kobayashi T, Harleton E, Sievert G, Balke CW, Feinmark SJ, and Solaro RJ et al. (2008) Tyrosine phosphorylation modifies protein kinase C delta-dependent phosphorylation of cardiac troponin I. *J Biol Chem* **283**:22680–22689.
- Takata A, Kawasaki H, Iwayama Y, Yamada K, Gotoh L, Mitsuyasu H, Miura T, Kato T, Yoshikawa T, and Kanba S (2011) Nominal association between a polymorphism in DGKH and bipolar disorder detected in a meta-analysis of East Asian case-control samples. *Psychiatry Clin Neurosci* **65**:280–285.
- Tang H, Shirai H, and Inagami T (1995) Inhibition of protein kinase C prevents rapid desensitization of type 1B angiotensin II receptor. *Circ Res* **77**:239–248.
- Tewson PH, Quinn AM, and Hughes TE (2013) A multiplexed fluorescent assay for independent second-messenger systems: decoding GPCR activation in living cells. *J Biomol Screen* **18**:797–806.
- Thangaraju A and Sawyer GW (2011) Comparison of the kinetics and extent of muscarinic M1-M5 receptor internalization, recycling and downregulation in Chinese hamster ovary cells. *Eur J Pharmacol* **650**:534–543.
- Toullec D, Pianetti P, Coste H, Bellevergue P, Grand-Perret T, Ajakane M, Baudet V, Boissin P, Boursier E, and Loriolle F et al. (1991) The bisindolylmaleimide GF 109203X is a potent and selective inhibitor of protein kinase C. *J Biol Chem* **266**:15771–15781.
- Usachev YM, DeMarco SJ, Campbell C, Strehler EE, and Thayer SA (2002) Bradykinin and ATP accelerate Ca(2<sup>+</sup>) efflux from rat sensory neurons via protein kinase C and the plasma membrane Ca(2<sup>+</sup>) pump isoform 4. *Neuron* **33**:113–122.
- Usachev YM, Marsh AJ, Johanns TM, Lemke MM, and Thayer SA (2006) Activation of protein kinase C in sensory neurons accelerates Ca<sup>2+</sup> uptake into the endoplasmic reticulum. *J Neurosci* **26**:311–318.
- van Baal J, de Widt J, Divecha N, and van Blitterswijk WJ (2012) Diacylglycerol kinase  $\theta$  counteracts protein kinase C-mediated inactivation of the EGF receptor. *Int J Biochem Cell Biol* **44**:1791–1799.
- van Blitterswijk WJ and Houssa B (2000) Properties and functions of diacylglycerol kinases. *Cell Signal* **12**:595–605.
- Venkatachalam K, van Rossum DB, Patterson RL, Ma HT, and Gill DL (2002) The cellular and molecular basis of store-operated calcium entry. *Nat Cell Biol* **4**:E263–E272.
- Violin JD, Zhang J, Tsien RY, and Newton AC (2003) A genetically encoded fluorescent reporter reveals oscillatory phosphorylation by protein kinase C. *J Cell Biol* **161**:899–909.
- Weber H, Kittel-Schneider S, Gessner A, Domschke K, Neuner M, Jacob CP, Buttenschon HN, Boreatti-Hümmer A, Volkert J, and Herterich S et al. (2011) Cross-disorder analysis of bipolar risk genes: further evidence of DGKH as a risk gene for bipolar disorder, but also unipolar depression and adult ADHD. *Neuropsychopharmacology* **36**:2076–2085.
- Yamada K, Sakane F, Imai Si, Tsushima S, Murakami T, and Kanoh H (2003) Regulatory role of diacylglycerol kinase gamma in macrophage differentiation of leukemia cells. *Biochem Biophys Res Commun* **305**:101–107.
- Yosifova A, Mushiroda T, Kubo M, Takahashi A, Kamatani Y, Kamatani N, Stoianov D, Vazharova R, Karachanak S, and Zaharieva I et al. (2011) Genome-wide association study on bipolar disorder in the Bulgarian population. *Genes Brain Behav* **10**:789–797.
- Young LT, Li PP, Kish SJ, Siu KP, Kamble A, Hornykiewicz O, and Warsh JJ (1993) Cerebral cortex Gs alpha protein levels and forskolin-stimulated cyclic AMP formation are increased in bipolar affective disorder. *J Neurochem* **61**:890–898.
- Zeng Z, Wang T, Li T, Li Y, Chen P, Zhao Q, Liu J, Li J, Feng G, and He L et al. (2011) Common SNPs and haplotypes in DGKH are associated with bipolar disorder and schizophrenia in the Chinese Han population. *Mol Psychiatry* **16**:473–475.

**Address correspondence to:** Mark J. Zylka, Department of Cell Biology & Physiology, 5109D NRB, CB #7545, The University of North Carolina at Chapel Hill, Chapel Hill, NC 27599-7545. E-mail: zylka@med.unc.edu